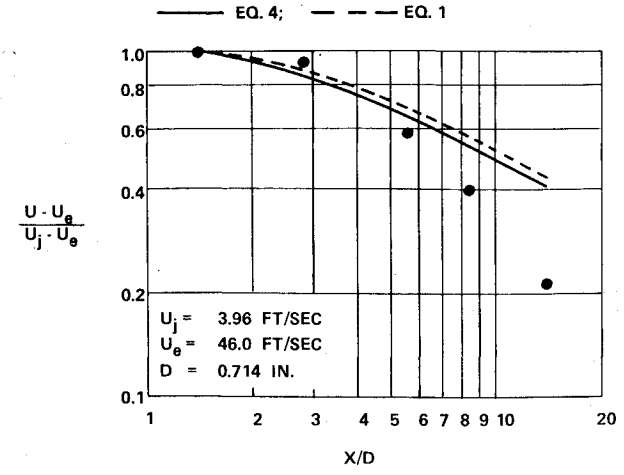

Fig. 6 Centerline velocity decay, Ref. 12, calculations started at $X/D = 1.4$.

shows somewhat better correlation of the data obtained with Eq. (1) than either the Prandtl model or Eq. (4).

On the other hand the usefulness of these comparisons made in Ref. 1 and shown in Fig. 3a is questionable for two important reasons. First, all the data shown was not taken with the same nozzle diameter (both $D = 1.0$ in. and 0.25 in. were used), and also the primary and secondary velocities were not fixed, i.e., in series C, $U_j = 180$ fps; whereas, in series F, $U_j = 90$ fps. Therefore, using the data from two different experimental cases to compare against the predictions of single case assumes the flowfield to be similar. Second, Forstall[10] reported the initial boundary layers on the splitter plate significantly increased the mixing. This effect is not considered in either of these models. An assumption of similarity is not required if only data points obtained with a 0.25-in.-diam nozzle are used in Series E of the Forstall data. When this is done, as shown in Fig. 3b, Eq. (1) overestimates mixing by as much as 50%. This overestimation is not surprising since this case more closely approximates the quiescent jet condition, i.e., $U_j = 4U_e$.

Examination of Fig. 4 shows that Eq. (4) also gave good agreement with the data of Chriss,[11] i.e., a high speed subsonic hydrogen jet exhausting into a high speed subsonic air stream. Both models give reasonable agreement with the low speed wake like ($U_e > U_j$) data of Ref. 12 for constant density flows (Fig. 5) but neither model did well (Fig. 6) for flows where the central jet gas was Freon and the external stream was air. Further verification of the generality of Eq. (4) was shown by comparison with 17 cases as reported in Ref. 14.

Discussion

Inspection of Figs. 2–5 shows that in some cases Eqs. (1) and (4) have predicted a centerline velocity decay which differs from experiment by as much as 50%. Two possible sources of this poor correlation are: first, the implicit assumption of equilibrium, and second, the absence of radial variation in the models. Radial variation was found to be significant[15] for flows in the transition region such as the data of Chriss, in which large density variations exist across the jet.

It is felt that better prediction methods for the entire mixing region must include the effects of upstream history of the turbulence quantities, i.e., intensities and shear correlations. Since the upstream flowfield development is important, these prediction schemes should begin at least at the point at which mixing is initiated. This region contains information about splitter plate boundary layer profiles and preturbulence levels which is neither measured nor reported in available jet mixing data. It is strongly recommended that future investigations include these important parameters.

References

[1] Schetz, J. A., "Turbulent Mixing of a Jet in a Coflowing Stream," *AIAA Journal*, Vol. 6, No. 10, Oct. 1968, pp. 2008–2010; see also NASA-CR1382, July 1969.

[2] Schetz, J. A., "Analysis of the Mixing and Combustion of Gaseous and Particle Laden Jets in an Air Stream," AIAA Paper 69-33, New York, 1969.

[3] Harsha, P. T., "Free Turbulent Mixing: A Critical Evaluation of Theory and Experiment," Ph.D. dissertation, 1971, Univ. of Tennessee.

[4] Lee, S. C. and Harsha, P. T., "The Use of Turbulent Kinetic Energy in Free Mixing Studies," AIAA Paper 69-683, San Francisco, Calif., 1969.

[5] Nee, V. W. and Kovasznay, L. S. G., "Simple Phenomenological Theory of Turbulent Shear Flows," *The Physics of Fluids*, Vol. 12, No. 3, pp. 473–484.

[6] Eggers, J. M., "Velocity Profiles and Eddy Viscosities Distributions Downstream of a Mach 2.2 Nozzle Exhausting to Quiescent Air," TN 3601, Sept. 1966, NASA.

[7] Warren, W. R., Jr., "An Analytical and Experimental Study of Compressible Free Jets," Publ. 23-885, 1957, Univ. Microfilms Inc.

[8] Hinze, J. O., *Turbulence*, McGraw-Hill, New York, 1959.

[9] Schlichting, H., *Boundary Layer Theory*, 4th ed., McGraw-Hill, New York, 1960.

[10] Forstall, W., "Material and Momentum Transfer in Coaxial Gas Streams," Ph.D. thesis, 1949, MIT; also *Journal of Applied Mechanics*, 1950, pp. 399–408.

[11] Chriss, D. E., "Experimental Study of Turbulent Mixing of Subsonic Axisymmetric Gas Streams," AEDC-TR-68-133, Aug. 1968, Arnold Engineering Development Center, Tenn.

[12] Zawacki, T. S. and Weinstein H., "Experimental Investigations of Turbulence in the Mixing Region Between Coaxial Streams," CR-959, Feb. 1968, NASA.

[13] Eggers, J. M. and Torrence, M. G., "An Experimental Investigation of the Mixing of Compressible Air Jets in a Coaxial Configuration," TN 5315, July 1969, NASA.

[14] Zelazny, S. W. and Herendeen, D. L., "Eddy Viscosity in Quiescent and Coflowing Axisymmetric Jets," Rept. 9500-920187, June 1970, Bell Aerospace Co., Wheatfield, N. Y.

[15] Zelazny, S. W. and Morgenthaler, J. H., "Turbulent Transport Coefficient in Coflowing Streams," AIAA Paper 69-682, San Francisco, Calif., 1969.

Plane Stress Analysis of Two Rigid Circular Inclusions

THOMAS J. KIM* AND VIJAY G. UKADGAONKER†
University of Rhode Island, Kingston, R. I.

Introduction

THE problems of finding the stress field around an arbitrary hole in an infinite plane can be generally solved by mapping the given region into a unit circle via Schwartz-Christoffel transformation, and many recent studies have been reviewed extensively in the book by Savin.[1] However, this procedure becomes rather cumbersome for a hole with nonsmooth contour or one that is defined in a multiply connected region since the mapping function, in general, becomes an infinite series. To avoid an infinite number of terms,

Received February 23, 1971; revision received August 2, 1971.
Index categories: Structural Static Analysis; Optimal Structural Design.

* Assistant Professor of Mechanical Engineering and Applied Mechanics.

† Graduate Assistant; now at Lehigh University, Department of Mechanical Engineering and Mechanics.

many investigators truncate the terms after the initial two or three terms of the series which results in some distortion of the original shape of the hole. The computational difficulties arising in the elastostatics problems for the multiply connected region can be substantially eased by reducing the solution to a sequence of problems in simply connected domains. This can be accomplished by making some modifications to Schwarz's treatment[2] of the Dirichlet problem for the overlapping domain.

In this Note, Schwarz's alternating method is used to find the stress field induced by two rigid inclusions in an isotropic homogeneous infinite plate. Two rigid disks of different radii $a + \epsilon_1$ and $b + \epsilon_2$ are respectively inserted into the two circular holes of radii a and b, where ϵ is very small in its magnitude as compared to the radii. It is assumed that no slip occurs in the process of insertion such that the interaction between the disks and plate reduces to normal pressure on the edge of the disks and plate. The problem is defined in the complex z plane and the stress functions which are valid in the vicinity of each hole are obtained by successive approximation starting from each hole.

Analysis

Two-dimensional problems in the theory of elasticity in the absence of body forces are reduced to the determination of two complex stress functions $\phi(z)$ and $\psi(z)$ which are analytic in a given region. The stress components are expressed as[3]

$$\begin{aligned} \sigma_r + \sigma_\theta &= 4Re[\phi'(z)] \\ \sigma_\theta - \sigma_r + 2i\tau_{r\theta} &= 2e^{2i\theta}[\bar{z}\phi''(z) + \psi'(z)] \end{aligned} \tag{1}$$

where σ_r and σ_θ are the normal stress components and $\tau_{r\theta}$ is the shearing stress with reference to polar coordinates.

The stress functions $\phi(z)$ and $\psi(z)$ for an infinite region pierced by a circular hole of radius R are given as

$$\phi(z) = -\frac{1}{2\pi i}\int_L \frac{f(t)}{t - z}\,dt \tag{2}$$

$$\psi(z) = -\frac{1}{2\pi i}\int_L \frac{\langle f(t)\rangle}{t - z}\,dt - \frac{1}{2\pi i}\int_L \frac{\langle f(t)\rangle}{t}\,dt - \frac{R^2}{z}\phi'(z) \tag{3}$$

where $t = Re^{i\theta}$; $f(t)$ is the resultant stress on a prescribed boundary L; and $\langle f(t)\rangle$ is the conjugate of $f(t)$. If the stresses are given on the boundary L, the stress-boundary condition f can be expressed in terms of the complex stress functions as

$$f(t) = \phi(t) + t\langle\phi'(t)\rangle + \langle\psi(t)\rangle \text{ on } L \tag{4}$$

Now let the center of the hole c_1 in Fig. 1 be located at the origin of a complex z_1 plane. Then the corresponding stress-boundary conditions can be obtained from Eqs. (2-4) by replacing z by z_1, t by $t_1 = a\exp(i\theta_1)$, R by a, and L by c_1. Similarly, the stress functions corresponding to the hole c_2, which has the center at the origin of z_2 plane, are determined by replacing z by z_2, t by $t_2 = b\exp(i\theta_2)$, R by b, and L by c_2.

Table 1 Maximum hoop stress at F for varying b/a and c/a

	σ_θ at $(r_1,\theta_1) = (a,0)$		$d = (c - a - b)/a$	
b/a	$d = 0.1$	$d = 0.5$	$d = 1$	$d = 2$
1	$1p + 3.3058q$	$1p + 1.7778q$	$1p + 1q$	$1p + 0.4444q$
1.5	$1p + 3.5156q$	$1p + 2.2500q$	$1p + 1.4400q$	$1p + 0.7347q$
2	$1p + 3.6281q$	$1p + 2.5600q$	$1p + 1.7778q$	$1p + 1q$
2.5	$1p + 3.6982q$	$1p + 2.7778q$	$1p + 2.0408q$	$1p + 1.2346q$
3	$1p + 3.7461q$	$1p + 2.9388q$	$1p + 2.2500q$	$1p + 1.4400q$
3.5	$1p + 3.7809q$	$1p + 3.0526q$	$1p + 2.4198q$	$1p + 1.6198q$
4	$1p + 3.8073q$	$1p + 3.1605q$	$1p + 2.5600q$	$1p + 1.7778q$

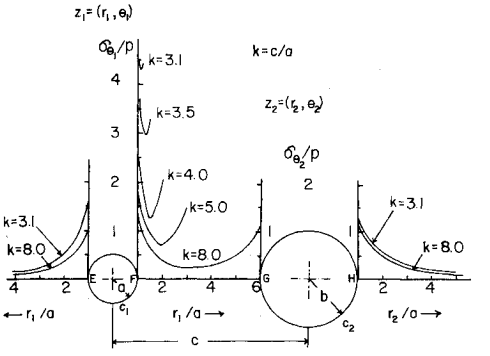

Fig. 1 Stress distribution along the line of symmetry for $p = q$ and $b = 2a$.

First and Second Approximations

For an infinite plate containing only one hole of radius a, stress functions can be determined from Eqs. (2) and (3) which yields

$$\phi_1(z_1) = 0, \quad \psi_1(z_1) = -pa^2/z_1 \tag{5}$$

where $p = 2\epsilon_1 G/a$ (G is shear modulus of the plate), and the subscript 1 indicates a boundary of the region in the neighborhood of which the stress functions are valid. Similarly the stress functions for a hole c_2 (in the absence of c_1) take the forms

$$\phi_2(z_2) = 0, \quad \psi_2(z_2) = -qb^2/z_2 \tag{6}$$

where $q = 2\epsilon_2 G/b$.

The stress functions determined in the forms of Eqs. (5) and (6) yield the normal stresses which are inversely proportional to the radial distance squared, and these, for sufficiently large distance $c = c_L$, will give the exact solution to the given problem. However, for a certain distance c, such that $a + b \leq c < c_L$, these might be considered as the first approximation in which no mutual effect of the holes are taken in consideration.

The second approximation which is valid near the hole c_2 is derived by starting from the hole c_1 as follows. The solution in Eq. (5) is obtained in the absence of the hole c_2. Thus, by piercing the second hole c_2 at $z_1 = c$ (with inclusion) the stress field around c_2, which is caused by c_1, will be disturbed. Furthermore, the boundary condition on c_2 will not take the form of $f(t_2) = -qt_2$ due to the presence of the residual stresses. In order to adjust the stress-boundary condition on c_2, the corrected stress resultant on c_2 is obtained in the form

$$f_2(t_2) = -qt_2 - f(t_2) \tag{7}$$

where $f(t_2)$ is determined by translating the stress function in Eq. (5) to $z_1 = c$ using the transformation $z_1 = z_2 + c$. Since the stress components in the first part of the Eq. (1) is invariant under a translation, the corresponding stress function $\phi_1(z_1)$ is also invariant, i.e.,

$$\phi_{12}(z_2) = \phi_1(z_1) = 0 \tag{8}$$

where subscript 12 indicates the translation from z_1 to z_2. However, the function $\psi_1(z_1)$ is not invariant under the translation of the origin and ψ_{12} takes the form

$$\psi_{12}(z_2) = \psi_1(z_1) + c\phi_{12}'(z_2) = -pa^2/(z_2 + c) \tag{9}$$

From Eqs. (4, 8, and 9)

$$\begin{aligned} f(t_2) &= \phi_{12}(t_2) + t_2\langle\phi_{12}'(t_2)\rangle + \langle\psi_{12}(t_2)\rangle \\ &= -pa^2t_2/(b^2 + ct_2) \end{aligned} \tag{10}$$

and from Eq. (7)

$$f_2(t_2) = -qt_2 + pa^2t_2/(b^2 + ct_2) \tag{11}$$

Substituting the corrected stress resultant $f_2(t_2)$ and its conjugate $\langle f_2(t_2)\rangle$ into the Eqs. (2) and (3), and evaluating the complex integrals the corresponding stress functions are determined as

$$\phi_{22}(z_2) = -pa^2b^2/c(cz_2 + b^2) \tag{12}$$

$$\psi_{22}(z_2) = pa^2/c - qb^2/z_2 - pa^2b^4/z_2(cz_2 + b^2) \tag{13}$$

Thus, the stress functions which are valid in the neighborhood of c_2 are expressed as the sum of the transformed stress functions and the adjusted ones, and they are

$$\phi_2(z_2) = \phi_{12}(z_1) + \phi_{22}(z_2) = -\frac{pa^2b^2}{c(cz_2 + b^2)}$$

$$\psi_2(z_2) = -pa^2/(z_2 + c) + pa^2/c - qb^2/z_2 - pa^2b^2/z_2(cz_2 + b^2)^2 \tag{14}$$

The stress functions corresponding for the second approximation which is valid in the vicinity of c_1 can be obtained by a similar analysis starting from the hole c_2, and they are

$$\phi_1(z_1) = -qa^2b^2/c(cz_1 - a^2)$$

$$\psi_1(z_1) = -qb^2/(z_1 - c) - pa^2/z_1 - qb^2/c - qa^4b^2/z_1(cz_1 - a^2)^2 \tag{15}$$

The higher order approximations[4] can be obtained by a similar process described above with no mathematical difficulties encountered. It can easily be shown that the successive approximation constructed in this manner converges, but the rapidity of convergence will depend on the magnitude of the parameters a,b,c,ϵ_1, and ϵ_2.

Numerical Results and Discussion

The numerical results for the distribution of stresses in the plate were obtained with the aid of digital computer for the case of $b = 2a$. In Fig. 1, the variation of the hoop stress along the line of symmetry is illustrated graphically for various spacing ($k = c/a$) of the holes. It shows that the high-stress concentrations always occur at the point F on c_1 and G on c_2, and their magnitudes increase substantially as the holes get closer for the fixed radius ratio $b = 2a$. For instance, the stress at F is 4.75 times higher than that of the single inclusion for the case of $k = 3.1$ and $p = q$. As the spacing of the holes increases, the stress pattern rapidly converges to unity which is the exact result[4] obtained in a single hole solution. Thus, for practice one can set a certain limit on the value of k beyond which the mutual effect of inclusions is not significant. The limit can be determined from Table 1, in which the maximum hoop stress at F is expressed in terms of p and q, by varying the radius ratio, ϵ_1 and ϵ_2. It also shows that the maximum stress concentration at F is much more sensitive to the distances between the holes than moderate change in the radius ratio.

References

[1] Savin, G. N., *Stress Concentration Around Holes*, Pergamon Press, New York, 1961.

[2] Sokolinkoff, I. S., *Mathematical Theory of Elasticity*, 2nd ed., McGraw-Hill, New York, 1956, pp. 313–327.

[3] Muskhelishvili, N. I., *Some Basic Problems of the Mathematical Theory of Elasticity*, Groninger-Holland, 1953, pp. 138–218.

[4] Ukadgaonker, V. G., "Two Unequal Circular Inclusions in an Infinite Plate," M.S. thesis, 1970, Univ. of Rhode Island, Kingston, R. I.

Establishment Time of Laminar Separated Flows

MICHAEL S. HOLDEN

Cornell Aeronautical Laboratory Inc., Buffalo, N. Y.

I. Introduction

THE time required to establish steady flow in complex regions of viscous interaction and flow separation remains an important question despite over a decade of measurements in facilities with short run times such as shock tubes, shock tunnels, and piston and arc driven facilities. Measurements in shock tubes and shock tunnels at Cornell Aeronautical Laboratory (CAL) have indicated that separated regions can take from 100 μsec to several msec to become fully established. Definitive measurements of the time establishment process in piston and arc driven facilities have in general not been possible because of the length and complexity of the starting process. For the set of measurements reported here a 40-ft driver section was fitted to the CAL 48 ft tunnel to give long test times at low incident Mach numbers. Figure 1 shows the test times available when the tunnel is operated under tailored interface conditions with 20- and 40-ft drivers. The boundary marking the appearance of the driver gas in the test section was determined from gas sampling techniques and heat transfer measurements ahead and in the base separated region. At incident shock Mach numbers of less than 2.5, we obtain running times greater than 20 msec.

II. Experimental Measurement

Base flow measurements

In the experimental studies of base flows, pressure and heat transfer measurements were made around spheres with diameters of 2, 6, 9, and 12 in., at Mach numbers from 6 to 8.5, unit Reynolds numbers from 2×10^6 to 9×10^6, and T_w/T_o from 0.1 to 0.4. Typical pressure and heat transfer records ahead and in the base regions are shown in Fig. 2. For the conditions shown the nozzle flow and the attached boundary layers are fully established within 1.5 msec. The gross structure of the separated region is established first, with the pressure in the neighborhood of the separation point taking the longest time to stabilize; the fine structure, as indicated by the heat transfer close to the rear stagnation

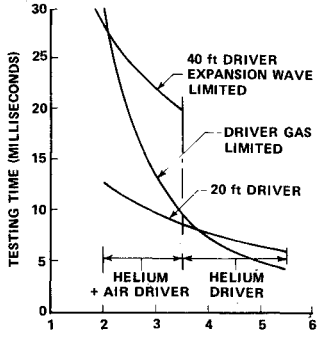

Fig. 1 Test time for tailored interface operation of 48 in. shock tunnel.

* Received April 22, 1971; revision received July 23, 1971. This experimental investigation was supported on CAL Feasibility Investigation Account 7152-442. Some measurements used in defining the time establishment of regions of shock wave-boundary layer interaction were taken in earlier experimental programs under Contracts AF 33(615)-1205 and F33615-67-C-1298 for the Air Force Aerospace Research Laboratories.

Index category: Nonsteady Aerodynamics.

* Principal Aerodynamicist, Aerodynamic Research Department. Associate Member AIAA.